Invited Paper

Progress of a compact microwave clock based on atoms cooled with a diffractive optic

Rachel Elvin, Gregory W. Hoth, Michael Wright, Ben Lewis, Alan Bregazzi, Brendan Keliehor, Aidan S. Arnold, Paul F. Griffin, and Erling Riis[a]

[a]Dept. of Physics, SUPA, University of Strathclyde, Glasgow, G4 0NG, UK

ABSTRACT

An atomic clock based on a compact source of cold atoms and coherent population trapping (CPT) is an encouraging goal for future low-volume atomic frequency references. Our experiment seeks to investigate the performance of such a system by applying CPT in a high-contrast lin⊥lin polarisation scheme to our ^{87}Rb grating magneto optical trap (GMOT) apparatus. In this paper, we report on our progress of improving short-term stability of our cold-atom CPT apparatus. Our recent measurements have shown a short-term stability of $5 \times 10^{-11}/\sqrt{\tau}$, with the ability to average down for times $\tau > 100\,\mathrm{s}$.

Keywords: Coherent Population Trapping. Grating Magneto-Optical Trap. Microwave Atomic Clock. Laser Cooling. Cold-Atoms. Micro-fabricated Grating Chips.

1. INTRODUCTION

In recent years, the miniaturisation of quantum sensors such as magnetometers and atomic clocks has become increasingly popular. In particular, clock experiments adopting the coherent population trapping (CPT) technique[1,2] as a means of interrogation have seen considerable improvement over the years. Devices built around this technique apply the microwave interrogation in an optical probe in order to measure the clock frequency. This probe consists of a bi-chromatic field with two components separated by the clock frequency that traps the atoms in a non-interacting superposition (or a dark state) between the ground states. The measured response is a narrow resonance feature in the probe transmission through the atoms. Applying the probe in a Raman-Ramsey pulsed scheme can then significantly reduce measurement linewidths and probe-induced frequency shifts.[3,4]

Whilst CPT alone was important for the development of miniature vapour cell atomic clocks,[5,6] several high-contrast methods have since been developed that boost the transmission signal and therefore the performance of frequency references based on CPT. The techniques were adapted to capitalise on constructive interference of dark state resonances[7] and have been applied in both thermal-atom and laser-cooled CPT clock experiments. They include polarisation schemes such as lin||lin,[8,9] lin⊥lin[4,10,11] or $\sigma^+ - \sigma^-$[12,13] and a pulsed technique known as push-pull optical pumping (PPOP).[14]

In terms of performance, CPT clocks based on alkali atoms in vapour cells have been under development for a long time, demonstrating short-term stabilities at the $10^{-13}\sqrt{\tau}$ level.[14] However, in the long-term the stability of these devices is predominately limited by frequency drifts. On the other hand, cold-atom CPT clocks have shown short-term stabilities on the order of $10^{-11}\sqrt{\tau}$ with the ability to average down to $10^{-13}\sqrt{\tau}$.[15] Despite the higher instability observed in cold-atom CPT clocks, the long-term behaviour is encouraging, the cold atoms having provided an elegant test-bed for probe induced systematic shifts of the clock frequency.

With the goal of a compact cold-atom frequency reference in mind, the next problem to tackle is the large, complicated laser-cooling apparatus. In addition to the few commercial cold-atom clocks now settling into the market,[16,17] a promising approach to reducing apparatus volume is the grating magneto-optical trap (GMOT). A single incident beam on a micro-fabricated grating chip replaces the standard counter-propagating beams, creating the required trapping volume from the diffracted first orders and maximising optical access to the atomic cloud. In this presentation, we review the recent performance of our lin⊥lin CPT clock based on a ^{87}Rb GMOT.[11,18] In Sec. 2, the GMOT apparatus is introduced and briefly described, followed by a summary of the

photonics.phys.strath.ac.uk/atom-optics

Optical, Opto-Atomic, and Entanglement-Enhanced Precision Metrology II, edited by Selim M. Shahriar, Jacob Scheuer, Proc. of SPIE Vol. 11296, 1129609 · © 2020 SPIE
CCC code: 0277-786X/20/$21 · doi: 10.1117/12.2552587

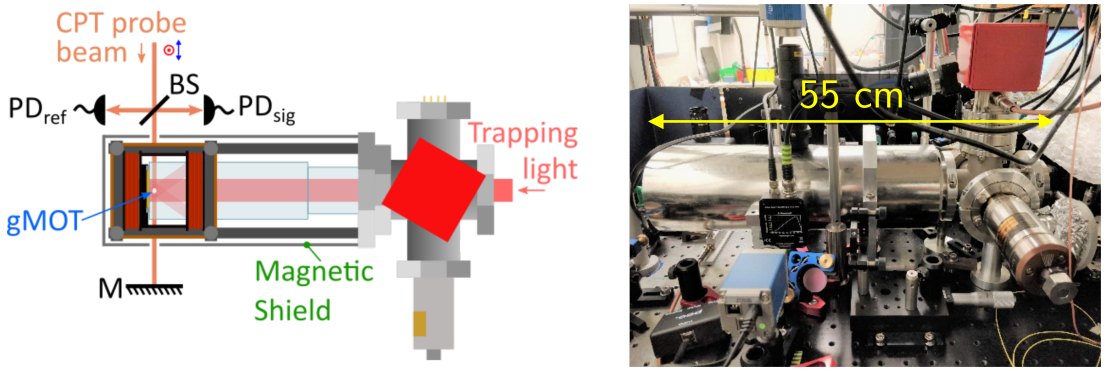

Figure 1. a) A schematic of the GMOT apparatus. The grating chip is mounted securely to the end facet of the glass cell. Quadrupole anti-helmholtz coils for trapping and Earth field- cancelling coils in the helmholtz configuration are also mounted to the vacuum chamber. The CPT probe is passed through holes in the magnetic shield. b) A photograph of the GMOT apparatus with its magnetic shield installed, and an approximate size of the chamber is labelled.

optical bench we used to generate the lin⊥lin laser-field from one laser in Sec. 3. In Sec. 4, we present our most recent measurements of the clock performance with the short-term frequency stability of the apparatus. Finally, we conclude our recent measurements and discuss the direction of our cold-atom CPT apparatus.

2. GMOT APPARATUS

In this section, we briefly describe our laser-cooling apparatus. To investigate the performance of a cold-atom lin⊥lin CPT clock, our experiment is based on a ^{87}Rb grating magneto-optical trap (GMOT) that has also been described in previous work.[18–20] For the GMOT apparatus, a micro-fabricated grating chip is securely mounted to the end facet of a compact glass vacuum cell. The grating holder, along with anti-Helmholtz and Helmholtz coils for trapping and cooling are attached to the chamber for ease of alignment or movement of the system. The 20 mm^2 chip we use in this experiment is comprised of three linear gratings that are arranged in a symmetrical triangle, referred to in previous publications as a TRI-grating.[21]

The GMOT requires a single beam of trap and repump light collimated to a waist-size comparable with the size of the grating, such that the diffracted first orders balance with the input beam to create a gem-shaped trapping volume. Two separate external-cavity diode lasers (ECDLs) are used to prepare the trap and repumping light for ^{87}Rb, where the former is red-detuned from the $F = 2 \rightarrow F' = 3$ transition and the latter is resonant with the $F = 1 \rightarrow F' = 2$ transition on the D_2 line of ^{87}Rb. The light is transferred to the vacuum chamber using a common single-mode optical fibre, where the beam is then expanded, collimated and circularly polarised before it reaches the grating chip. As is shown in Fig. 1, the entire apparatus is enclosed in a cylindrical mu-metal shield to suppress the ambient magnetic field at the location of the atoms. With the current GMOT system, 10^6 atoms are typically loaded and then cooled to sub-Doppler temperatures of around 20 μK.

3. APPARATUS FOR LIN⊥LIN CPT

To optically probe the ground state hyperfine splitting of the ^{87}Rb atoms, we adopt CPT in a lin⊥lin polarisation scheme and apply the interrogation in a Raman-Ramsey pulsed sequence.[4,11,22] For lin⊥lin CPT on the D_1 line of ^{87}Rb, we use the $F' = 2$ as our common hyperfine excited state in order to drive the double-lambda transition structure drawn in Fig. 2 a). This particular scheme maxmimises our measured Ramsey fringe amplitude and pumps atoms into a dark state with minimal sensitivity to ambient magnetic fields.[22,23]

The lin⊥lin CPT fields are generated from a single 795 mn ECDL and an electro-optical modulator (EOM), operating at a frequency close to the hyperfine ground state splitting frequency, $f_{\mathrm{HFS}} \sim 6.8$ GHz. A schematic of the optical bench can be found in Fig. 2 b). The ECDL is locked using saturated absorption spectroscopy (SAS) with a frequency offset set by an acousto-optical modulator (AOM), not shown in the figure. The frequency of this AOM is also used to set our one-photon detuning, which is kept constant throughout the experiment. The output beam from the ECDL is split into two paths, where one is sent through the fibre-coupled EOM and the

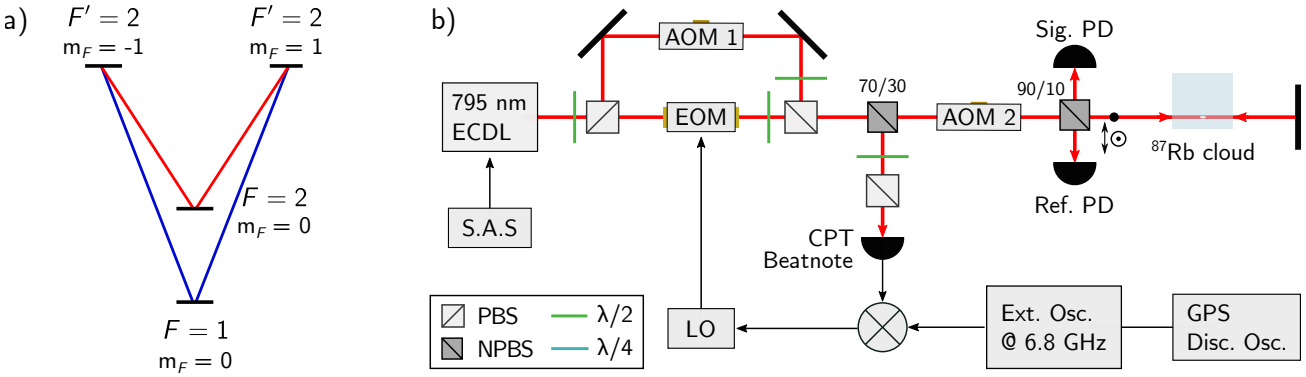

Figure 2. a) The double-Λ CPT transisions on the D_1 line of the ^{87}Rb for pumping into the desired dark state between the $|F = 1, m_F = 0\rangle$ and $|F = 2, m_F = 0\rangle$ ground state levels, using the hyperfine $F' = 2$ as the common excited state. b) A schematic of the optical bench that is used to generate the optical fields to drive the lin⊥lin CPT polarisation scheme from one ECDL.

other through an AOM (AOM 1 in the figure). After the beams are re-combined, a second AOM (AOM 2) is used to bring the light from the AOM 1 path onto resonance with the $F = 2 \rightarrow F' = 2$ transition and a single sideband from the EOM path onto resonance with the $F = 1 \rightarrow F' = 2$ transition.

This method allows us to produce two laser modes, orthogonally polarised and resonant with the ^{87}Rb CPT transitions shown in Fig. 2 a). Generating the CPT from a single laser allows for relative simplicity and provides good phase coherence between the CPT frequency components. Splitting the path also introduces some disadvantages, such as noise on the relative phase between the CPT components. This is caused by the separated paths and degrades the short-term stability of our apparatus. The extra noise was suppressed by implementing a phase-locked loop (PLL), as shown in the schematic in Fig. 2 b). For this PLL we compared a CPT beatnote to an external frequency source in order to provide feedback for the local oscillator (LO) which in turn drives the EOM. Further details on this investigation can be found in previous work.[18] In addition, the probe contains extra frequency components, such as the carrier in the EOM path, that are off-resonance with the transitions in Fig. 2 a). This will be under investigation in the future.

The second AOM (AOM 2 in the figure) is also used to switch the intensity of the probe light, allowing us to generate the pulses for the Ramsey-CPT sequence.[4] After this AOM and the pick-off for the CPT beat-note, the probe beam is fibre-coupled into a single-mode fibre to ensure good mode overlap between the combined beams. The probe is then sent through the cold rubidium cloud in a double-passed configuration. The atoms are prepared in the GMOT and then cooled in an optical molasses. After cooling we apply two pulses of the CPT light, separated by a variable free evolution time, T. In the first pulse, atoms are pumped into the dark state between the $|F = 1, m_F = 0\rangle$ and $|F = 2, m_F = 0\rangle$ ground state levels. The second pulse is used to detect the phase difference between the LO frequency and atomic resonance during the free evolution time. Measuring the transmission of the CPT beam as the frequency of our LO is scanned allows us to obtain the CPT spectrum or Ramsey fringes. Common-mode intensity noise on our signal is suppressed by normalising the recorded transmission from one photodiode (Sig. PD in Fig. 2 b)) with a second photodiode, Ref. PD in Fig. 2 b). In addition to the noise suppression from the reference photodiode, a second stage of normalisation is applied to the detected Ramsey fringes. Using the dynamic nature of the detection pulse, we take the ratio of the integrated transmission at the beginning of the pulse and the integrated transmission at the end of the pulse.[9,15]

4. PERFORMANCE

In this section, we review the performance of lin⊥lin CPT with our ^{87}Rb GMOT experiment. Using the sequence described above, 10^6 atoms were prepared in the GMOT with a loading time of ~ 300 ms, and our free evolution time was set to $T = 10$ ms. In the lin⊥lin CPT scheme we typically measure a CPT contrast of approximately 65%, plotted in Fig. 3 (a). We estimate the CPT contrast by comparing the depth of the absorption feature, A_{abs}, to the height of the CPT transmission peak, A_{cpt}, as is also labelled in Fig. 3 (a).

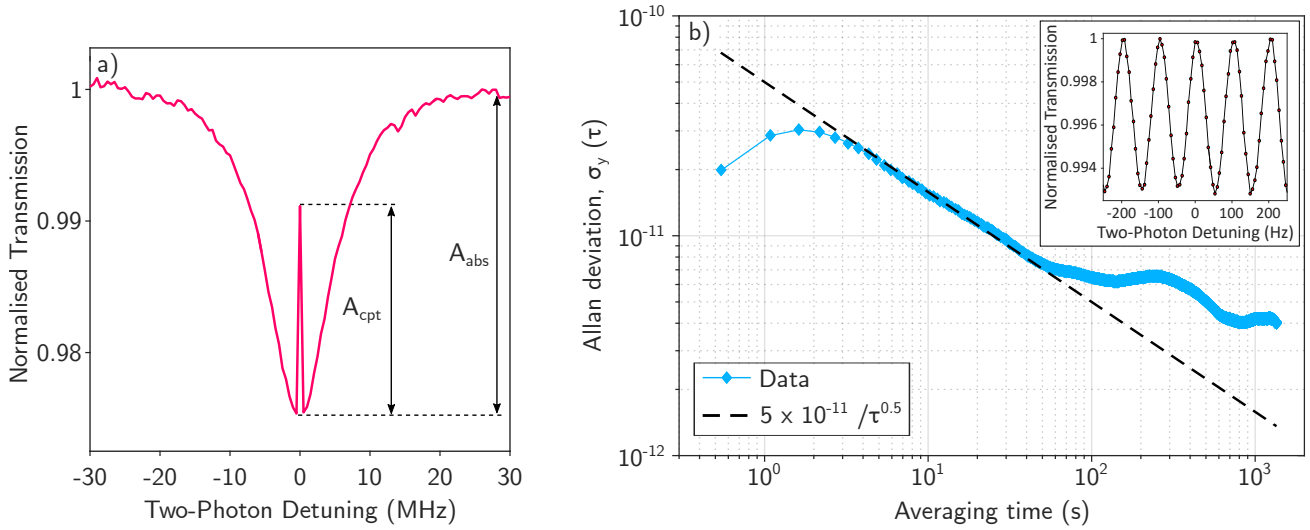

Figure 3. a) Measured optical CPT spectrum as the two-photon detuning, set by the frequency of the EOM, is scanned 30 MHz on either side of the CPT resonance. The spectrum has been normalised to the off-resonant wings of the absorption dip, which has a depth of A_{abs}. This data corresponds to a CPT contrast of $\sim 65\%$, calculated from the ratio of the transmission peak height to the absorption height, A_{cpt}/A_{abs}. b) Measured Allan deviation curve of the cold-atom lin⊥lin CPT experiment, taken with a free-evolution time of $T = 10$ ms. A straight line is drawn to show the $1/\sqrt{\tau}$ coefficient. (Inset) A typical Ramsey fringe from a free evolution time of $T = 10$ ms. Each data point is a one run of the experiment sequence.

Using the double-ratio to suppress intensity noise on the detected Ramsey fringes, we obtain a single-shot SNR of about 50 for a free-evolution time of $T = 10$ ms. At this Ramsey time, a fringe pattern with width $\delta = 50$ Hz is obtained, shown in the inset of Fig. 3 (b). To quantify the performance of our apparatus as a clock, we measure the short-term frequency stability of the system. In this measurement the LO is set to alternate between $\pm\delta/2$, corresponding to the sides of the central Ramsey fringe, where each shot is a single run of the experiment sequence. Using the linear regions on the fringe as a frequency discriminator, we can then measure the frequency difference between the average LO output frequency and the atomic resonance frequency. In our apparatus, all frequency sources related to the clock part of the experiment are referenced to a GPS-disciplined oscillator.

Figure 3 (b) shows the measured Allan deviation curve of the frequency deviations for the CPT clock apparatus. In this experiment, frequency steers are applied to the LO between shots of the experiment sequence that are calculated using the measured transmission at the sides of the fringe. The black dashed line is plotted to represent the $1/\sqrt{\tau}$ line, from which we can observe a short-term stability of $5 \times 10^{-11}/\sqrt{\tau}$ for this set of data. The measured instability is higher than we have presented in previous work. We believe this is due to the replacement of the atom recapture sequence[18] with a longer MOT loading time. From an internal investigation this was ascribed to light-leakage from an AOM used for switching the trap light, causing a light-shift of the central fringe that was difficult to suppress without installing a mechanical shutter. Installing the shutter extinguished the leaked light during the Ramsey-CPT sequence, but also limited how quickly the sequence could be run. In future, we will investigate the re-implementation of atom re-capture.

In previous publications, the short-term stability of our apparatus appeared to plateau and, in some cases, largely deviate after an averaging time of around $\tau = 10$ s. As addressed in Sec. 2 and 3, upgrades that include the installation of a mechanical shutter in the trap beam and magnetic shielding around the vacuum cell, were made to the experiment that are intended to effectively improve stability in the long-term. The Allan deviation curve in Fig. 3 (b) shows relatively smaller stability bumps around $\tau = 100$ s, attributed to temperature drifts, that highlight a clear improvement on our previous measurements. For now, this is still an ongoing investigation.

5. CONCLUSION

Following our previous investigations into the performance of lin⊥lin CPT with a GMOT, we have measured a short-term stability of approximately $5 \times 10^{-11}/\sqrt{\tau}$ in a locked configuration. Despite the higher instability, we find these measurements encouraging as the behaviour of the Allan deviation curves shows an improvement to previous limits to our measured stability. For future work, it is our intention to continue to use the frequency stability to investigate other CPT probe induced shifts such as the Doppler shift and AC-stark shifts. It will be useful to thoroughly investigate the latter due to the extra frequency components in our CPT probe light.

Acknowledgment

We acknowledge financial support from EPSRC through the UK Quantum Technology Hub for Sensors and Metrology (EP/M013294/1). The data supporting this publication can be accessed at this link: https://doi.org/10.15129/4e8b9f40-937f-414f-ac43-400ad2713d05

REFERENCES

[1] Vanier, J., "Atomic Clocks Based on Coherent Population Trapping: A Review," *Applied Physics B* **81**, 421–442 (Aug. 2005).

[2] Miletic, D., Affolderbach, C., Hasegawa, M., Boudot, R., Gorecki, C., and Mileti, G., "Ac stark-shift in cpt-based cs miniature atomic clocks," *Applied Physics B* **109**(1), 89–97 (2012).

[3] Hemmer, P. R., Shahriar, M. S., Natoli, V. D., and Ezekiel, S., "Ac stark shifts in a two-zone raman interaction," *Journal of the Optical Society of America B* **6**(8), 1519 (1989).

[4] Zanon, T., Guerandel, S., de Clercq, E., Holleville, D., Dimarcq, N., and Clairon, A., "High Contrast Ramsey Fringes with Coherent-Population-Trapping Pulses in a Double Lambda Atomic System," *Physical Review Letters* **94**, 193002 (May 2005).

[5] Knappe, S., Shah, V., Schwindt, P. D. D., Hollberg, L., Kitching, J., Liew, L.-A., and Moreland, J., "A Microfabricated Atomic Clock," *Applied Physics Letters* **85**, 1460–1462 (Aug. 2004).

[6] Cash, P., Krzewick, W., Machado, P., Overstreet, K. R., Silveira, M., Stanczyk, M., Taylor, D., and Zhang, X., "Microsemi Chip Scale Atomic Clock (CSAC) Technical Status, Applications, and Future Plans," in [*2018 European Frequency and Time Forum (EFTF)*], 65–71 (Apr. 2018).

[7] Taichenachev, A. V., Yudin, V. I., Velichansky, V. L., and Zibrov, S. A., "On the unique possibility of significantly increasing the contrast of dark resonances on the D_1 line of ^{87}Rb," *Journal of Experimental and Theoretical Physics Letters* **82**, 398–403 (Oct. 2005).

[8] Blanshan, E., Rochester, S. M., Donley, E. A., and Kitching, J., "Light Shifts in a Pulsed Cold-Atom Coherent-Population-Trapping Clock," *Physical Review A* **91**, 041401 (Apr. 2015).

[9] Esnault, F.-X., Blanshan, E., Ivanov, E. N., Scholten, R. E., Kitching, J., and Donley, E. A., "Cold-atom Double-Λ Coherent Population Trapping Clock," *Physical Review A* **88**, 042120 (Oct. 2013).

[10] Xi, C., Guo-Qing, Y., Jin, W., and Ming-Sheng, Z., "Coherent Population Trapping-Ramsey Interference in Cold Atoms," *Chinese Physics Letters* **27**, 113201 (Nov 2010).

[11] Elvin, R., Hoth, G. W., Wright, M., Lewis, B., McGilligan, J. P., Arnold, A. S., Griffin, P. F., and Riis, E., "Cold-atom clock based on a diffractive optic," *Opt. Express* **27**, 38359–38366 (Dec 2019).

[12] Liu, X., Yudin, V. I., Taichenachev, A. V., Kitching, J., and Donley, E. A., "High Contrast Dark Resonances in a Cold-Atom Clock Probed with Counter-Propagating Circularly Polarized beams," *Applied Physics Letters* **111** (Nov. 2017).

[13] Elgin, J. D., Heavner, T. P., Kitching, J., Donley, E. A., Denney, J., and Salim, E. A., "A cold-atom beam clock based on coherent population trapping," *Applied Physics Letters* **115**(3), 033503 (2019).

[14] Abdel Hafiz, M., Coget, G., Yun, P., Guérandel, S., de Clercq, E., and Boudot, R., "A High-Performance Raman-Ramsey Cs Vapor Cell Atomic Clock," *Journal of Applied Physics* **121**, 104903 (Mar. 2017).

[15] Liu, X., Ivanov, E., Yudin, V. I., Kitching, J., and Donley, E. A., "Low-Drift Coherent Population Trapping Clock Based on Laser-Cooled Atoms and High-Coherence Excitation Fields," *Physical Review Applied* **8**, 054001 (Nov. 2017).

[16] Hendricks, R. J., Ozimek, F., Szymaniec, K., Nagórny, B., Dunst, P., Nawrocki, J., Beattie, S., Jian, B., and Gibble, K., "Cs Fountain Clocks for Commercial Realisations - an Improved and Robust Design," in [*IEEE Transactions on Ultrasonics, Ferroelectrics, and Frequency Control*], 1–1 (Oct. 2018).

[17] Pelle, B., Desruelle, B., Szmuk, R., and Holleville, D., "Cold-Atom-Based Commercial Microwave Clock at the 10^{-15} Level," in [*2017 Joint Conference of the European Frequency and Time Forum and IEEE International Frequency Control Symposium (EFTF/IFCS)*], 479–480 (Jul. 2017).

[18] Hoth, G. W., Elvin, R., Wright, M., Lewis, B., Arnold, A. S., Griffin, P. F., and Riis, E., "Towards a compact atomic clock based on coherent population trapping and the grating magneto-optical trap," in [*Optical, Opto-Atomic, and Entanglement-Enhanced Precision Metrology*], *Optical, Opto-Atomic, and Entanglement-Enhanced Precision Metrology* (2019).

[19] McGilligan, J. P., Griffin, P. F., Elvin, R., Ingleby, S. J., Riis, E., and Arnold, A. S., "Grating chips for quantum technologies," *Scientific Reports* **7**(1) (2017).

[20] Hoth, G. W., Elvin, R., Wright, M. W., Lewis, B., Arnold, A. S., Griffin, P. F., and Riis, E., "Impact of laser frequency noise in coherent population trapping with cold atoms," in [*2019 Joint Conference of the European Frequency and Time Forum and IEEE International Frequency Control Symposium (EFTF/IFCS)*], *IEEE Proceedings, IFCS-EFTF* (2019).

[21] Nshii, C. C., Vangeleyn, M., Cotter, J. P., Griffin, P. F., Hinds, E. A., Ironside, C. N., See, P., Sinclair, A. G., Riis, E., and Arnold, A. S., "A surface-patterned chip as a strong source of ultracold atoms for quantum technologies," *Nature Nanotechnology* **8**(5), 321–324 (2013).

[22] Elvin, R., Hoth, G. W., Wright, M. W., McGilligan, J. P., Arnold, A. S., Griffin, P. F., and Riis, E., "Raman-Ramsey CPT with a Grating Magneto-Optical Trap," in [*2018 European Frequency and Time Forum (EFTF)*], *European Frequency and Time Forum (EFTF)* , 61–64 (Apr. 2018).

[23] Warren, Z., Shahriar, M. S., Tripathi, R., and Pati, G. S., "Experimental and Theoretical Comparison of Different Optical Excitation Schemes for a Compact Coherent Population Trapping Rb Vapor Clock," *Metrologia* **54**(4), 418 (2017).